Journal of Nuclear Medicine, published on April 28, 2016 as doi:10.2967/jnumed.115.168575

Left ventricular function assessment using two different cadmium zinc telluride cameras compared to gamma camera with cardiofocal collimators: dynamic cardiac phantom study and clinical validation.

Alban Bailliez[1,2,3], MD, PhD; Olivier Lairez[4], MD, PhD; Charles Merlin[5], MD; Nicolas Piriou[6], MD; Damien Legallois[3,7], MD; Tanguy Blaire[1,2,3], MD; Denis Agostini[3,8], MD, PhD; Frederic Valette[6], MD; Alain Manrique[3,8], MD, PhD.

[1] Nuclear Medicine, IRIS, Polyclinique du Bois, Lille, France,

[2] Nuclear Medicine, UF 5881, Groupement des Hôpitaux de l'Institut Catholique de Lille, Lomme, France

[3] Normandie Université - EA4650, Caen, France

[4] Nuclear Medicine, CHU de Toulouse, Toulouse, France

[5] Nuclear Medicine, Centre Jean Perrin, Clermont-Ferrand, France

[6] Nuclear Medicine, CHU de Nantes, France

[7] Cardiology, CHU de Caen, France

[8] Nuclear Medicine, CHU de Caen, Caen, France

Corresponding Author : Alban Bailliez, MD, PhD Nuclear Medicine Department IRIS, 144 avenue de Dunkerque, Polyclinique du Bois, 59000 LILLE, France, Tel : (+33) 320 001 655, Fax : (+33) 320 098 010, Email : abailliez@gmail.com.

Short Title : CZT VS CARDIOFOCAL CAMERA IN LV FUNCTION

Word counts:

Abstract: 282 words.

Article: 4799 words (including the abstract, tables, legends, and references)

Keywords: CZT, myocardial perfusion imaging, left ventricular function, wall thickening, dynamic phantom, cardiofocal collimators.

ABSTRACT

This study compared the DNM-530c (GE Healthcare) and DSPECT (Biosensors International) using cadmium zinc telluride (CZT) detectors to a conventional Anger camera with cardiofocal collimators (Symbia IQ, Siemens) for left ventricular (LV) function assessment in phantom and patients. **Methods:** The Amsterdam gated (AGATE) dynamic cardiac phantom (Vanderwilt techniques, Boxtel, The Netherlands) was used. Eighteen acquisitions were processed on each CZT and Anger (IQ SPECT) camera. The total number of counts varied from 0.25 kcts to 1.5 Mcts within a myocardial VOI. Ejection fraction (EF) was set to 33%, 45% or 60%. Volumes, ejection fraction (LVEF), regional wall thickening and motion (17-segment model) were assessed using QGS (Cedars-Sinaï). One hundred and twenty patients with low pretest likelihood of coronary artery disease and normal stress perfusion SPECT were retrospectively analyzed to provide the normal limits for EDV, ESV, EF and regional function for each camera model. **Results:** In the phantom study, for each EF value, volumes were higher using the DNM-530c and DSPECT cameras compared to IQ SPECT, resulting in decreased but more accurate LVEF (all $P<0.001$). In clinical data, body-surface indexed ventricular volumes were higher using the DNM-530c compared to DSPECT and IQ SPECT [respectively EDVi (mL/m^2): 40.5±9.2, 37±7.9 and 35.8±6.8 ($P<0.001$), ESVi (mL/m^2): 12.5±5.3, 9.4±4.2 and 8.3±4.4 ($P<0.001$)], resulting in a significantly decreased LVEF (%): 70.3±9.1 vs. 75.2±8.1 vs. 77.8±9.3 ($p <0.001$). **Conclusion:** New CZT cameras yielded different results of global LV function compared to Anger camera with cardiofocal collimators. In our study, LV volumes were higher using the DNM 530c compared to DSPECT and IQ SPECT, leading to decreased LVEF in normal subjects. These differences should be taken into account in clinical practice and warrant the collection of specific normal database.

INTRODUCTION

Myocardial perfusion imaging is extensively used in patients with known or suspected coronary artery disease. In addition, the measurement of left ventricular ejection fraction (LVEF), end diastolic (EDV) and end systolic volumes (ESV) using gated single photon computed tomography (SPECT) has been widely validated in comparison to other imaging techniques (*1,2*) and is commonly used for prognosis assessment and clinical decision making (*3*). Moreover, it has been demonstrated that the normal limits of left ventricular (LV) function are gender-specific but do not depend on tracer or acquisition camera when using conventional Anger cameras (*4*) suggesting equivalency for patient management.

New cadmium-zinc-telluride (CZT) dedicated gamma cameras revealed a new step in SPECT myocardial perfusion imaging. These cameras led to a reduced imaging time (*5*) and patients radiation exposure (*6,7*) but are not equivalent in terms of count sensitivity and spatial resolution, leading to images with different sharpnesses and contrast-to-noise ratios in clinical practice (*8*). Previous publications have validated the performance and results of these cameras versus conventional Anger camera in clinical practice (*9,10*) but recent data demonstrated that quantitative gated SPECT using CZT cameras overestimates left ventricular volumes, leading to lower LVEF values in normal patients compared to Anger models (*11*). This is likely related to the increased spatial resolution, a condition that also significantly impacts on the assessment of segmental wall motion and thickening (*12,13*). Alternatively, IQ SPECT with multifocal collimators, can be plugged-in on multipurpose cameras, offering a favorable performance regarding sensitivity and contrast-to-noise ratio when compared with conventional Anger cameras equipped with low-energy and high-resolution collimators (*14*).

As commercially available CZT cameras and IQ SPECT systems have different characteristics in terms of sensitivity and spatial resolution, it remains unclear whether the type of these new cameras may impact on the assessment of LV volumes and ejection fraction. Consequently, the aim of this study was to perform a head-to-head comparison of left ventricular function assessment using commercially available CZT and IQ SPECT systems with a dynamic cardiac phantom, and to confirm the phantom-based results by a retrospective analysis of data acquired in patients with low pretest likelihood of coronary artery disease.

MATERIALS AND METHODS

Gamma cameras and collimation systems

We used successively (i) a Discovery NM 530c (Alcyone, GE Healthcare, Milwaukee, WI, USA) equipped with a multiple pinhole collimator and 19 stationary CZT detectors which simultaneously image 19 cardiac views, each detector being composed of pixelated 5-mm thick (matrix 70 x70; pixel size 2.46 x 2.46 mm) elements (*15*) (ii) a DSPECT (Biosensors International) operating with 9 mobile blocks of pixelated CZT detectors (pixel size 2.46 x 2.46 mm) associated with a wide-angle square-hole tungsten collimator, recording a total of 120 projections by each block (*16*) and (iii) a IQ SPECT system with a high-sensitivity astigmatic collimator involving a convergent geometry for the image center and parallel holes for the edges connected to a Symbia camera (Siemens Medical Solutions, Erlangen, Germany), using a circular rotation (28-cm radius) and centered on the heart (128x128 matrix) (*14*). All SPECT dataset (phantom and patients) were acquired and reconstructed using the parameters currently recommended for clinical routine by each manufacturer, leading to a reconstructed pixel size of 4 x 4 x4, 4.92 x 4.92 x 4.92, and 4.8 x 4.8 x 4.8 mm respectively for Discovery NM 530c (DNM), DSPECT, and IQ SPECT. No attenuation correction was performed.

Dynamic Phantom study

We used the Amsterdam gated (AGATE) dynamic phantom (Vanderwilt techniques, Boxtel, The Netherlands) as a reference for volumes and LVEF measurements (*17*). This phantom is a realistic 3D water-filled torso with two thin membranes simulating endocardial and epicardial walls with known ventricular volumes and ejection fraction (Fig. 1). The lumen between these membranes was filled with a pertechnetate solution (50 kBq/mL) simulating a myocardial wall. The cardiac phantom stroke volume is controlled by a programmable adjustable pumping system, and an ECG triggered signal is produced at a constant heart rate. Eighteen acquisitions were performed on each CZT camera and IQ SPECT, with counting stop conditions varying from 0.25 Kcts, 0.5 Kcts, 0.75 Kcts, 1 Mcts, 1.25 Mcts and 1.5 Mcts within a myocardial VOI. LVEF was set by the adjustable pumping system (17) to 33% and 45% to mimic LV dysfunction or to 60% to simulate normal LV function. The acquisition parameters were as follows: 70 x 70 matrix for the DNM system, 64 x 64 for the DSPECT with a total of 120 projections recorded by each block in the heart area being defined on a short prescan acquisition (*18*) and 128 x 128 matrix with 30 projections over 180° and 30 seconds per projection for the Anger IQ SPECT camera. The energy window was 140 keV ± 10% for all cameras.

Clinical data

We retrospectively analyzed post-stress acquisitions acquired in 120 consecutive patients referred to our Nuclear Medicine departments for a routine evaluation of myocardial perfusion with low pretest likelihood of coronary artery disease and normal stress only perfusion SPECT. Image dataset from Discovery NM were collected at Clinique du Bois (n=40, Lille, France), from DSPECT at Centre Hospitalier Universitaire de Caen (n=20, Caen, France) and Centre Jean Perrin (n=20, Clermont-Ferrand, France), and from IQ SPECT at Centre Hospitalier Universitaire de Nantes (n=20, Nantes, France) and Centre Hospitalier Universitaire Rangueil (n=20, Toulouse, France). Dicom stored dataset from 10 men and 10 women were retrieved for each camera and for both ^{99m}Tc-sestamibi and ^{99m}Tc-tetrofosmin to provide the normal limits for ventricular ejection EDV, ESV and LVEF, regional motion and thickening for each camera model. For all cameras, we used the reconstruction parameters as recommended by each vendor. For the DNM model, a Butterworth postprocessing filter (frequency, 0.37; order, 7) was applied to the reconstructed axial slices, which were subsequently reformatted in the standard cardiac axis for analysis. For the DSPECT, a specific algorithm for iterative reconstruction (4 iterations) is used to compensate for the collimator-related loss in spatial resolution (*16*) and IQ SPECT images were routinely reconstructed using a 3-dimensional iterative algorithm (6 iterations, 4 subsets)with correction for the geometry of the astigmatic collimator (Flash 3D) and a post-reconstruction filter (Gaussian, FWHM 8.4 mm). Ventricular volumes were indexed to body area for each patient (EDVi and ESVi) and patients' characteristics were collected from hospital records. All reconstructed dataset were stored in dicom format and subsequently processed by the QGS package (QGS 2008, Cedars Sinai, Los Angeles, CA) running on a Spectrum Dynamics workstation (Caesarea, Israel) and using a 17-segment model for regional myocardial wall thickening and motion analysis (*19*). All images were anonymized, and our ethics committee (Comité de Protection des Personnes Nord-Ouest III, Caen, France) approved this retrospective study and the requirement to obtain informed consent was waived.

Statistical Analysis

Continuous variables are presented as mean ± standard deviation. The Shapiro–Wilk test of normality was used to assess the normality of continuous variables. We used a multivariate analysis of variance (MANOVA) with post-hoc comparison of means (Tukey's test) or Kruskal-Wallis test when appropriate for global comparison between the three

cameras. The reproducibility between the Discovery NM, DSPECT and IQ SPECT for the measurement of EDV, ESV, and LVEF using the Agate phantom was tested using one-way random intraclass correlation coefficients (*20*). All statistical analyses were performed using R software (R Foundation for Statistical Computing, version 3.1.2, Vienna, Austria). A P-value < 0.05 was considered statistically significant.

RESULTS

Phantom study

The mean values of overall EDV, ESV, and LVEF, thickening and motion obtained using the Agate phantom with DNM 530c, D-SPECT and IQ SPECT are shown in Fig. 2. Measured phantom volumes were higher and EF lower using the DNM 530c compared to DSPECT and IQ SPECT. Using the phantom set up with a normal ventricular function (EF= 60%) or decreased LVEF (EF= 45% or 33%), there was a significant difference between cameras for EDV, ESV and EF (all P-values <0.05, see Fig. 2). There was no impact of count statistics on EDV, ESV and EF, whatever the camera model.

Clinical data

GLOBAL LEFT VENTRICULAR FUNCTION. Data obtained from 60 men (mean age 57.7±10.9 y) and 60 women (mean age 63.1±13.3 y) without evidence of heart disease were retrospectively assessed. As for phantom data, normal LV volumes were higher using the DNM 530c compared to DSPECT and IQ SPECT, respectively EDVi (mL/m^2): 40.5±9.2 vs. 37±7.9 vs. 35.8±6.8 (global P-value <0.001), ESVi (mL/m^2): 12.5±5.3 vs. 9.4±4.2 vs. 8.3±4.4 (global P-value <0.001), resulting in a significantly decreased LVEF (%): 70.3±9.1 vs. 75.2±8.1 vs. 77.8±9.3 (global P-value <0.001). For ESVi, EDVi and LVEF, MANOVA showed a significant effect of sex and camera (P<0.05). No effect of tracer (^{99m}Tc-tetrofosmin vs. ^{99m}Tc-sestamibi) was observed (p=NS), and clinical data from each tracer were pooled together for subsequent analyses. Results are presented in Fig. 3 and the mean values of EDVi, ESVi, and LVEF obtained from each camera according to gender are shown in Table 1.

SEGMENTAL WALL THICKENING AND MOTION. The assessment of segmental left ventricular function yielded lower mean values with the DNM 530c compared to DSPECT and IQ SPECT. Mean values for motion were respectively: 8.6±1.4 mm (DNM 530c), 9.1±1.5 mm (DSPECT) and 10.1±1.9 mm (IQ SPECT, global P-value <0.001), and mean values for thickening were 49.1±12.2 % (DNM 530c), 56.9±13 % (DSPECT) and 58±15.1 % (IQ SPECT, global P-value <0.05). Results are presented in Fig. 4.

DISCUSSION

The phantom study demonstrated that estimated LV volumes were different between the 3 systems, especially for ESV, leading to significant differences in normal or decreased LVEF values. The estimated volumes were increased when assessed using CZT camera, likely due to a better spatial resolution. The phantom study further indicated overestimations of normal LVEF values, particularly when using the IQ SPECT system. In patients, the normal values of left ventricular function were dependant on the gender and the camera type.

Global left ventricular function

The effect of the type of camera on global and segmental function is likely related to spatial resolution. Imbert et al. (8) reported the following classification of measured central spatial resolution, in order of performance: Discovery NM 530c (6.7 mm), DSPECT (8.6 mm) and IQ SPECT (15.0 mm). As shown in Fig. 2, our results in the phantom study suggested that the overestimation of LVEF was a function of spatial resolution, the overestimation being dramatically limited when using CZT cameras compared to IQ SPECT. The QGS algorithm used in this study works in three-dimensional space and is also limited by spatial resolution. Germano et al. early reported that a decrease in spatial resolution causes a reduction in estimated LV volumes (*21*). When the end-systolic cavity size approaches the spatial resolution of the system, the partial volume effect induces a blurring effect at the myocardial wall edges and QGS miscalculates the endocardial surface, leading to smaller volume estimation. Our findings also showed that the increased spatial resolution of CZT-based cameras, by minimizing the partial volume effect, resulted in increased volume measurements.

LV volume measurement may also be affected by reconstruction parameters (*22*), filtering and zooming (*23*), and absolute ventricular size (*24*). Clinical and simulation studies have previously reported an underestimation of the LV volume,

especially in small hearts (*23*,*25*). As the magnitude of underestimation depends on ventricle size, the relative effect is different on EDV and ESV calculations, leading to an overestimation of LVEF. Nakajima et al. (*25*) generated a set of mathematical simulations assuming an arbitrary resolution (15.7, 12.1, 9.2, 7.5 and 6.9 mm in full-width at half-maximum). In this latter study, the authors demonstrated that the measured-to-true volume ratio was optimized by a higher resolution in numerical simulations. In addition, they also showed in a pediatric population that using a zoom during acquisition resulted in the same effect on volume assessment. These data suggested that factors favoring spatial resolution, as reconstruction filters with a high cut-off frequency, high system resolution and appropriate zooming may improve gated SPECT quantification.

Sensitivity, contrast to noise ratio, photon scatter and energy resolution may also impact on volumes and function assessment. Previous phantom and clinical studies reported a 3-fold improved sensitivity with IQ SPECT, about 4-fold with Discovery NM 530c, and nearly 7-fold with DSPECT, and demonstrated different sharpness profiles measured in patients perfusion SPECT (*8*,*15*). Photon scatter correction and compensation techniques based on energy windowing have been documented for improving image quality and volume measurements (*26*,*27*). In particular, scattered photons in the main photopeak have a greater impact in smaller hearts than in large hearts (*28*). Although CZT cameras offer a high energy resolution (*15*), the scatter fraction remains similar to what observed with conventional Anger cameras (*18*). Thus, it remains unclear whether the increased resolution could participate to the increased image sharpness with CZT cameras, a condition leading to an easy and accurate detection of myocardial edges resulting in increased ventricular volumes compared to Anger camera.

In patients, the assessment of left ventricular volumes and ejection fraction has been validated against cardiac magnetic resonance (CMR) (*12*,*13*,*29*). Using a DNM 530c and the same software package, Giorgetti et al. (*29*) found excellent correlations with the CMR volumes for both EDV ($r = 0.92$) and ESV ($r = 0.95$) but with a significant underestimation (mean differences: EDV: -33.2 ± 26 mL; ESV: -17.9 ± 20 mL; $p < 0.001$). However, LVEF was highly correlated between CZT and CMR ($r = 0.91$) with similar values (49 ± 16 % vs. 51 ± 15 in their population for DNM 530c vs. CMR respectively). Cochet et al. (*13*) found similar results and further demonstrated that bias between CZT and CMR for the measurement of ESV (but not of EDV or LVEF) was greater in patients exhibiting moderate-to-severe defects. To our knowledge, there is no data comparing IQ SPECT to CMR for assessing LV function. However, our findings in patients without evidence of heart disease clearly showed that CZT cameras yielded increased LV volumes and decreased ejection fractions compared to IQ SPECT. As previously documented (*30*,*31*), gender-related differences were observed independently of the camera type. These results are in agreement with recent findings by Miao (*11*) who reported in a study

conducted in a normal population that measurements with a DNM 530c were significantly increased from those obtained by a dual-headed conventional gamma camera for EDVi and ESVi in both men and women. Our results further emphasized that the two commercially available CZT cameras provided different estimates of LV volumes, when assessed by means of QGS.

Segmental left ventricular function

Due to partial volume effect, a change in object size, as observed during myocardial contraction, results in changes in the apparent count density and is identified by a systolic increase in brightness. This method based on count density is widely used for assessing regional myocardial function with gated SPECT, but the exact quantification of the wall thickening remains limited (*32*). We previously demonstrated that the increased spatial resolution provided by CZT-based detectors may lead to an underestimation of regional myocardial wall thickening under hypertrophic conditions (*12*). In contrast, myocardial wall motion showed a higher agreement with cardiac MR than wall thickening (*12,13*). The present study demonstrated that regional myocardial wall thickening was decreased using the DNM 530c compared to the DSPECT, while there was no significant difference in terms of myocardial wall motion. These results support the usage of wall motion for the assessment of segmental ventricular function using CZT cameras.

STUDY LIMITATIONS

This study was performed using post-stress acquisitions, and does not provide information on rest perfusion scans. Due to the retrospective design of the patient study, we collected normal data from French centers that commonly use a stress only protocol (*33*). In these centers, patients with low likelihood of coronary artery disease and normal stress perfusion scans are discharged without performing the rest examination, resulting in a dramatically decreased radiation exposure. Consequently, this study was not able to assess the impact of camera type on transient ischemic dilation or myocardial stunning. Second, only a single reconstruction approach was used for each camera and it is uncertain whether or not our findings will apply to different reconstruction/filtering algorithms. Third, only one type of software was used (QGS). Methods based on statistical analysis of the distribution of count density, and not on edge detection, would significantly impact on volumes and EF measurements compared to QGS and other methods based on endocardial surface detection (*34,35)*. Therefore, the repeatability of our results using postprocessing methods avoiding edge detection is uncertain.

CONCLUSION

The different technical characteristics of commercially available CZT cameras (DNM 530c and DSPECT) and of a conventional camera equipped with an astigmatic collimator (IQ SPECT) resulted in different estimates of left ventricular function, when using QGS for 3-dimensional edge detection. These results confirm the need for gender- and camera-normative values for left ventricular function parameters.

DISCLOSURE SECTION

Alban Bailliez: no disclosure

Tanguy Blaire: no disclosure

Damien Legallois: no disclosure

Frederic Valette: no disclosure

Nicolas Piriou: no disclosure

Charles Merlin: no disclosure

Olivier Lairez: no disclosure

Denis Agostini: no disclosure

Alain Manrique: no disclosure

Acknowledgements

We are grateful to Dr Sylvie Petit, MD, Dr Mathilde Thelu, MD, Dr Dimitri Bellevre, MD and to the technologists in each institution (Lille, Toulouse, Nantes, Clermont-Ferrand and Caen) for their help and technical assistance.

References

1. Marcassa C, Bax JJ, Bengel F, et al. Clinical value, cost-effectiveness, and safety of myocardial perfusion scintigraphy: a position statement. *Eur Heart J*. 2008;29:557–563.

2. Hachamovitch R, Berman DS, Kiat H, Cohen I, Friedman JD, Shaw LJ. Value of stress myocardial perfusion single photon emission computed tomography in patients with normal resting electrocardiograms: an evaluation of incremental prognostic value and cost-effectiveness. *Circulation*. 2002;105:823–829.

3. Thomas GS, Miyamoto MI, Morello AP, et al. Technetium 99m sestamibi myocardial perfusion imaging predicts clinical outcome in the community outpatient setting. The Nuclear Utility in the Community (NUC) Study. *J Am Coll Cardiol*. 2004;43:213–223.

4. Ababneh AA, Sciacca RR, Kim B, Bergmann SR. Normal limits for left ventricular ejection fraction and volumes estimated with gated myocardial perfusion imaging in patients with normal exercise test results: influence of tracer, gender, and acquisition camera. *J Nucl Cardiol*. 2000;7:661–668.

5. Sharir T, Slomka PJ, Hayes SW, et al. Multicenter trial of high-speed versus conventional single-photon emission computed tomography imaging: quantitative results of myocardial perfusion and left ventricular function. *J Am Coll Cardiol*. 2010;55:1965–1974.

6. Verger A, Imbert L, Yagdigul Y, et al. Factors affecting the myocardial activity acquired during exercise SPECT with a high-sensitivity cardiac CZT camera as compared with conventional Anger camera. *Eur J Nucl Med Mol Imaging*. 2014;41:522–528.

7. Duvall WL, Croft LB, Ginsberg ES, et al. Reduced isotope dose and imaging time with a high-efficiency CZT SPECT camera. *J Nucl Cardiol*. 2011;18:847–857.

8. Imbert L, Poussier S, Franken PR, et al. Compared performance of high-sensitivity cameras dedicated to myocardial perfusion SPECT: a comprehensive analysis of phantom and human images. *J Nucl Med*. 2012;53:1897–1903.

9. Verger A, Djaballah W, Fourquet N, et al. Comparison between stress myocardial perfusion SPECT recorded with cadmium-zinc-telluride and Anger cameras in various study protocols. *Eur J Nucl Med Mol Imaging*. 2013;40:331–340.

10. Sharir T, Ben-Haim S, Merzon K, et al. High-speed myocardial perfusion imaging initial clinical comparison with conventional dual detector anger camera imaging. *JACC Cardiovasc Imaging*. 2008;1:156–163.

11. Miao TL, Kansal V, Glenn Wells R, Ali I, Ruddy TD, Chow BJW. Adopting new gamma cameras and reconstruction algorithms: Do we need to re-establish normal reference values? *J Nucl Cardiol*. 2015; doi:10.1007/s12350-015-0172-x.

12. Bailliez A, Blaire T, Mouquet F, et al. Segmental and global left ventricular function assessment using gated SPECT with a semiconductor Cadmium Zinc Telluride (CZT) camera: Phantom study and clinical validation vs cardiac magnetic resonance. *J Nucl Cardiol*. 2014;21:712–722.

13. Cochet H, Bullier E, Gerbaud E, et al. Absolute quantification of left ventricular global and regional function at nuclear MPI using ultrafast CZT SPECT: initial validation versus cardiac MR. *J Nucl Med*. 2013;54:556–563.

14. Caobelli F, Kaiser SR, Thackeray JT, et al. IQ SPECT allows a significant reduction in administered dose and acquisition time for myocardial perfusion imaging: evidence from a phantom study. *J Nucl Med*. 2014;55:2064–2070.

15. Bocher M, Blevis IM, Tsukerman L, Shrem Y, Kovalski G, Volokh L. A fast cardiac gamma camera with dynamic SPECT capabilities: design, system validation and future potential. *Eur J Nucl Med Mol Imaging*. 2010;37:1887–1902.

16. Gambhir SS, Berman DS, Ziffer J, et al. A novel high-sensitivity rapid-acquisition single-photon cardiac imaging camera. *J Nucl Med*. 2009;50:635–643.

17. Visser JJN, Sokole EB, Verberne HJ, et al. A realistic 3-D gated cardiac phantom for quality control of gated myocardial perfusion SPET: the Amsterdam gated (AGATE) cardiac phantom. *Eur J Nucl Med Mol Imaging*. 2004;31:222–228.

18. Erlandsson K, Kacperski K, van Gramberg D, Hutton BF. Performance evaluation of D-SPECT: a novel SPECT system for nuclear cardiology. *Phys Med Biol*. 2009;54:2635–2649.

19. Cerqueira MD, Weissman NJ, Dilsizian V, et al. Standardized myocardial segmentation and nomenclature for tomographic imaging of the heart: a statement for healthcare professionals from the cardiac imaging committee of the council on clinical cardiology of the American Heart Association. *Circulation*. 2002;105:539–542.

20. Shrout PE, Fleiss JL. Intraclass correlations: uses in assessing rater reliability. *Psychol Bull*. 1979;86:420–428.

21. Germano G, Kiat H, Kavanagh PB, et al. Automatic quantification of ejection fraction from gated myocardial perfusion SPECT. *J Nucl Med*. 1995;36:2138–2147.

22. Wright GA, McDade M, Martin W, Hutton I. Quantitative gated SPECT: the effect of reconstruction filter on calculated left ventricular ejection fractions and volumes. *Phys Med Biol*. 2002;47:99–105.

23. Véra P, Manrique A, Pontvianne V, Hitzel A, Koning R, Cribier A. Thallium-gated SPECT in patients with major myocardial infarction: effect of filtering and zooming in comparison with equilibrium radionuclide imaging and left ventriculography. *J Nucl Med*. 1999;40:513–521.

24. Nakajima K, Okuda K, Nyström K, et al. Improved quantification of small hearts for gated myocardial perfusion imaging. *Eur J Nucl Med Mol Imaging*. 2013;40:1163–1170.

25. Nakajima K, Taki J, Higuchi T, et al. Gated SPET quantification of small hearts: mathematical simulation and clinical application. *Eur J Nucl Med Mol Imaging*. 2000;27:1372–1379.

26. Manrique A, Hitzel A, Véra P. Impact of photon energy recovery on the assessment of left ventricular volume using myocardial perfusion SPECT. *J Nucl Cardiol*. 2004;11:312–317.

27. Galt JR, Cullom J, Garcia EV. Attenuation and scatter compensation in myocardial perfusion SPECT. *Semin Nucl Med*. 1999;29:204–220.

28. Hambye AS, Vervaet AM, Dobbeleir AA. Head-to-head comparison of uncorrected and scatter corrected, summed and end diastolic myocardial perfusion SPECT in coronary artery disease. *Nucl Med Commun*. 2004;25:347–353.

29. Giorgetti A, Masci PG, Marras G, et al. Gated SPECT evaluation of left ventricular function using a CZT camera and a fast low-dose clinical protocol: comparison to cardiac magnetic resonance imaging. *Eur J Nucl Med Mol Imaging*. 2013;40:1869–1875.

30. Sharir T, Kang X, Germano G, et al. Prognostic value of poststress left ventricular volume and ejection fraction by gated myocardial perfusion SPECT in women and men: gender-related differences in normal limits and outcomes. *J Nucl Cardiol*. 2006;13:495–506.

31. Gebhard C, Stähli BE, Gebhard CE, et al. Gender- and age-related differences in rest and post-stress left ventricular cardiac function determined by gated SPECT. *Int J Cardiovasc Imaging*. 2014;30:1191–1199.

32. Danias PG, Ahlberg AW, Travin MI, et al. Visual assessment of left ventricular perfusion and function with electrocardiography-gated SPECT has high intraobserver and interobserver reproducibility among experienced nuclear cardiologists and cardiology trainees. *J Nucl Cardiol*. 2002;9:263–270.

33. Hesse B, Tägil K, Cuocolo A, et al. EANM/ESC procedural guidelines for myocardial perfusion imaging in nuclear cardiology. *Eur J Nucl Med Mol Imaging*. 2005;32:855–897.

34. Véra P, Koning R, Cribier A, Manrique A. Comparison of two three-dimensional gated SPECT methods with thallium in patients with large myocardial infarction. *J Nucl Cardiol*. 2000;7:312–319.

35. Feng B, Sitek A, Gullberg GT. Calculation of the left ventricular ejection fraction without edge detection: application to small hearts. *J Nucl Med*. 2002;43:786–794.

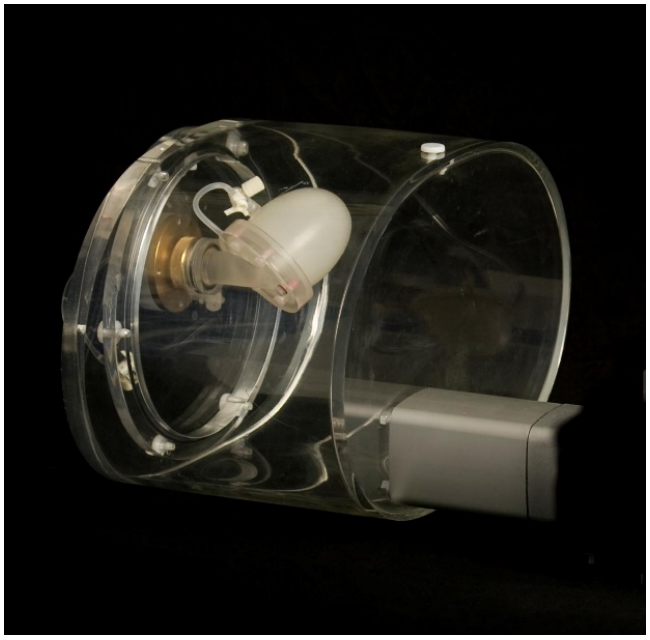

FIGURE 1: The Agate Dynamic Phantom.

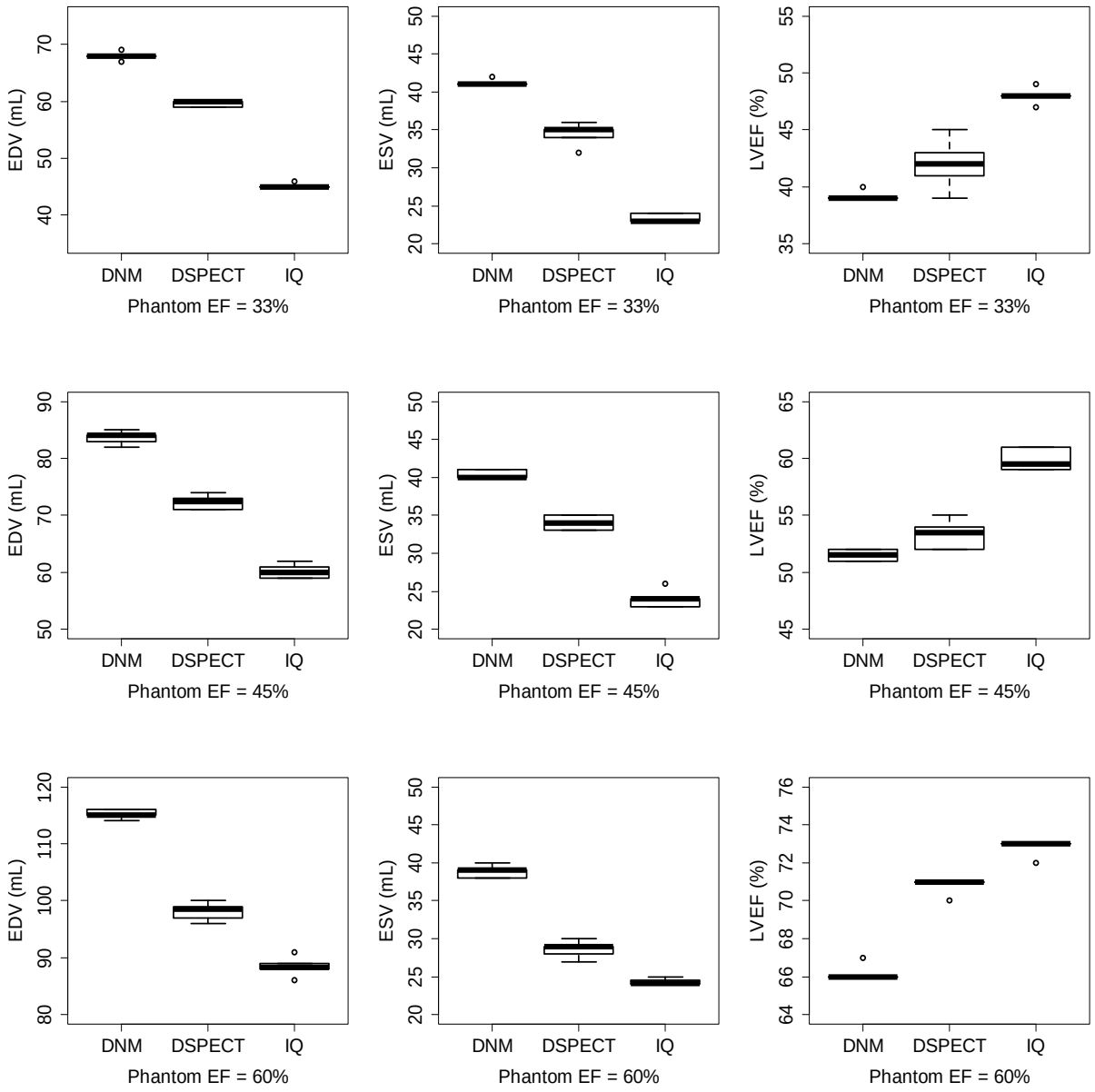

FIGURE 2: Comparison for phantom acquisitions of EDV, ESV and LVEF mean values for each camera for LVEF=33% (upper row), LVEF=45% and LVEF=60% (lower row). The horizontal line of Tukey's box marks the median of the samples while the hinges of each box represent the 25th and 75th percentiles. The error bars extending above and below each box show the range of values that fall within 1.5 s.d. of the hinges. All $P < 0.05$.

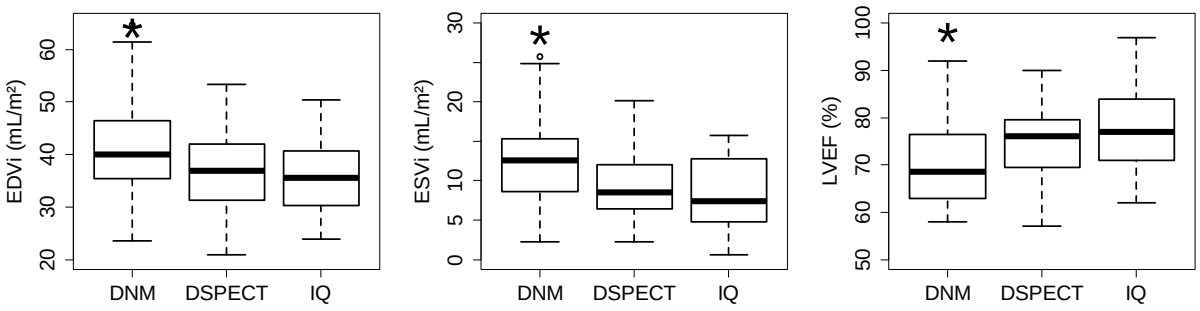

FIGURE 3: Comparison for patients study of EDVi (mL/m²), ESVi (mL/m²) and LVEF (%) for each camera. The horizontal line in the middle of a Tukey's box marks the median of the samples while the hinges of each box represent the 25th and 75th percentiles. The vertical lines extending above and below each box show the range of values that fall within 1.5 s.d. of the hinges. *P<0.05 for DNM vs. DSPECT and IQ.

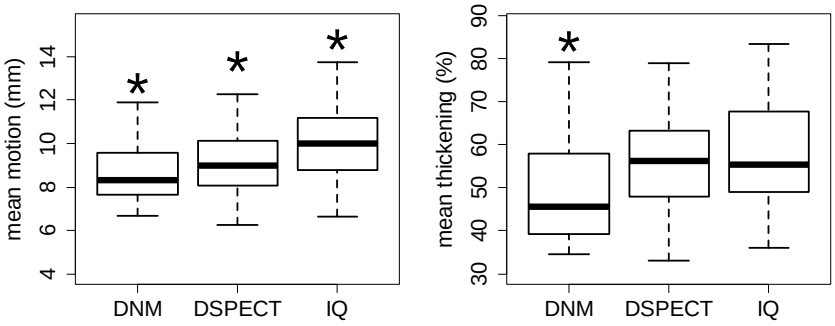

FIGURE 4: Comparison of wall motion (mm) and thickening (%) mean values obtained in patients with each camera (*P<0.05 vs. other cameras).

	DNM		DSPECT		IQ SPECT	
	Female	**Male**	**Female**	**Male**	**Female**	**Male**
Age (years)	64.4±14.6 (20-83)	59.5±9.7 (38-78)	61.6±14.2* (31-82)	51.6±10§ (30-65)	63.1±11.4 (33-81)	61.8±10.8§ (37-78)
BMI (kg/m²)	27.8±5.7 (19.5-42.5)	27.1±3 (22.5-32.4)	31.1±8.3 (19.5-45.9)	28.5±5.9 (21-45.9)	28.4±7.8 (18.7-50.7)	31.8±7.1 (18-43.8)
EDV (mL)	68±5.8* (43-100)	86.5±20.2‡ (48-138)	58.2±11.4* (41-83)	82.5±10.7 (62-105)	62.9±14.2* (39-87)	78.4±19.4‡ (50-115)
EDVi (mL/m²)	38±8.6 (23.8-56.1)	43.1±9.3‡ (23.5-64.7)	32.5±6.9* (20.9-46.8)	41.5±6.2 (30.5-53.3)	35±6.1 (26.1-45.9)	38.2±9.3‡ (24-55.4)
ESV (mL)	18.2±8.8* (4-35)	29.9±10.7‡ (15-58)	12.9±6.2* (4-26)	23.1±7.2 (13-37)	13.7±8.8 (1-30)	21.9±12.4‡ (5-55)
ESVi (mL/m²)	10.1±4.6* (2.2-19.3)	14.9±5‡ (8.4-25.8)	7.1±3.3* (2.2-13.2)	11.6±3.8 (7-20)	7.4±4.5 (1-15.7)	10.6±6‡ (3-25.7)
LVEF (%)	74.6±9.3* (58-92)	65.9±6.5†‡ (58-78)	78.5±7.6* (63-90)	71.9±7.4† (57-83)	79.6±10 (62-97)	73.8±10.1‡ (52-92)
Motion (mm)	9±1.5‡ (6.7-11.9)	8.3±1.1‡ (6.7-10.3)	9.4±1.5 (6.3-12.3)	8.7±1.4 (6.4-11.1)	10.6±2.2‡ (7-16.6)	9.4±1.7‡ (6.6-13.4)
Thickening (%)	53.8±13.4* (35.8-79.1)	44.4±8.9‡ (34.7-63.1)	58.9±13.3 (33-92.6)	54.9±12.7§ (35.2-79)	62.2±17.3 (36.9-113.1)	51.9±12.8‡§ (32-81.1)

TABLE 1: Clinical results for each camera model expressed as: mean±SD (min-max). * P< 0.05 vs. male gender using the same camera, † P<0.05 DNM vs. DSPECT,

‡ P<0.05 DNM vs. IQ SPECT, § P<0.05 DSPECT vs. IQ SPECT within the same gender.